

RESEARCH

Open Access



Nanoparticles derived from insect exoskeleton modulates NLRP3 inflammasome complex activation in cervical cancer cell line model

Rituparna Chakraborty¹, Ujjal Bose^{4*}, Goutam Pawaskar², Satish Rao Bola Sadashiva³ and Ritu Raval^{2,5*} 

*Correspondence:
ujjal.bose@manipal.edu; ritu.raval@manipal.edu

² Department of Biotechnology, Manipal Institute of Technology, Manipal Academy of Higher Education, Manipal 576104, Karnataka, India

⁴ Department of Pharmacology, Melaka Manipal Medical College, Manipal Academy of Higher Education, Manipal 576104, Karnataka, India

Full list of author information is available at the end of the article

Abstract

Background: Immune evasion is an important hallmark of cancer progression and tumorigenesis. Among the cancer types, cervical cancer has very high global prevalence, severely affecting female reproductive health. Its preponderance is also observed in the Indian health sector.

Results: The NLRP3 inflammasome, an intracellular complex regulates the innate immune activity and a variant gene of it has been significantly associated with cervical cancer development. We aimed to evaluate the potential role of our chitosan engineered nanoparticles (CSNP) and gallic acid conjugated chitosan (gCSNP), to modulate the NLRP3 inflammasome complex in cervical cancer cell lines to explore their novel physicochemical properties. The encapsulation of gallic acid (GA) with chitosan was performed using ion gelation method. The CSNP and gCSNP nanoparticles ranged between 155 and 181 nm as determined by zeta sizer. The conjugations were validated by FTIR and XRD analysis. In the cervical cell line model, CSNP suppressed NLRP3 inflammasome activation in contrast to gCSNP at higher doses.

Conclusion: In contrast to gCSNP, the CSNP not only demonstrated inhibitory effect on the expression of genes coding for the NLRP3 inflammasome complex (signal 1—priming), but also decreased relative expression of gene involved in the activation of NLRP3 inflammasome complex (signal 2—activation). Conjugation of gallic acid reversed the immunosuppressor mimicking action of CSNP in cervical cancer cell line. Future research can reveal the immunomodulatory mechanism of CSNP may have its translational significance as potential treatment strategies targeting immune evasion as an important hallmark of cancer.

Keywords: Chitosan nanoparticles, Gallic acid, NLRP3 inflammasome, HeLa 229cell line



Background

Cervical malignancy is the fourth most prevalent neoplasm globally and second most common among Indian women (Arbyn et al. 2020; Mishra et al. 2016). Inflammation induced through microbial or danger signals affects all stages of tumor development. The pro-inflammatory cytokines, IL-1 β and IL-6, are important mediators for inflammation-induced tumorigenesis (Moossavi et al. 2018). The NLRP3 inflammasome is a multimeric protein complex that regulates the innate immune activity through modulation of the production of pro-inflammatory cytokines. A variant NLRP3 gene has been significantly associated with cervical cancer development (Pontillo et al. 2016). However, the role of NLRP3 inflammasome activation in tumorigenesis, transformation and invasion, remains a conundrum (Moossavi et al. 2018). Activation of the NLRP3 inflammasome is a two-step process where microbial toxins or danger signals and ATP are necessary for inflammasome activation. There is a lack of adequate therapeutic strategies targeting key immune signaling pathways involving the inflammasome complex in cancer treatment.

Nanoparticles hold promise in offering a unique opportunity that increases the efficiency of cancer immunotherapy as well as ameliorates their toxic side-effects (Hamarsheh and Zeiser 2020; Park et al. 2018). We hypothesize that our engineered nanoparticles CSNP/gCSNP can prevent the outcome of the priming signal by inhibiting the expression of genes coding for the NLRP3 inflammasome complex proteins in human cervical epithelial adenocarcinoma cells. Furthermore, we aimed at studying the role of CSNP/gCSNP on the genes coding for the purinergic receptor (P2RX7) which functions as a major contributor in providing the second kick necessary for activating the NLRP3 inflammasome complex. Additionally, the study aimed at evaluating the effect of our engineered nanoparticles on the gene coding for pro-inflammatory cytokine IL1 β and its release from stimulated cervical cancer cells.

A pilot study by one of our co-investigators indicated a positive effect of chitosan-based nanoparticles and oligosaccharides on the anti-inflammatory cytokines, in the *in vivo* study conducted on the cyclophosphamide-treated mice model (Mudgal et al. 2019). As an extension of these findings, this study was undertaken to investigate the effect of chitosan nanoparticles on the NLRP3 inflammasome complex to establish the relationship between innate immunity, inflammation and disease progression in cervical cancer cell line model.

Cancer immunotherapy has come a long way to significantly augment conventional cancer therapy in recent years (Kruger et al. 2019; Sun 2017). Although NLRP3 inflammasome has been implicated both in tumorigenesis and as a response to antitumour therapy, it provides a lucrative target for cancer immunotherapy (Hamarsheh and Zeiser 2020; Kantono and Guo 2017; Karki and Kanneganti 2019). Hence the present study further investigated the multipronged potential of CSNP/gCSNP as a robust immune modulator in cervical cancer cells, to address the molecular mechanisms behind the activation of inflammasomes. Here, we not only targeted the expression of critical genes in the canonical pathway, but also the activation mechanism of the NLRP3 inflammasome complex in cervical cancer cells. Moreover, the present study aimed at exploring the possibilities of pharmacological potential of the CSNP nanoparticles and its modified form as gCSNP.

Materials and methods

Physicochemical characterization of engineered nanoparticles

The formulated nanoparticles (NP) were dissolved in an appropriate volume of HPLC-grade water and the average hydrodynamic diameter, polydispersity index (PDI) and zeta potential were estimated with ZetaSizer Nano ZS90 (Malvern Instruments Limited, UK) equipped with a 4.0 mW He–Ne laser. The detection angles of 90° and 120° were used for determination of: (a) size and PDI, and (b) the zeta potential of the synthesized nanoparticles, respectively. The FTIR spectra of CSNP, gCSNP and GA were recorded on a Jasco FT/IR-6300 Spectrometer equipped with a DR PRO410-M (Jasco, Japan) by scanning from 4000 to 500 cm^{-1} at a resolution of 4 cm^{-1} and analyzed using Microsoft Excel (Microsoft Office version 2016, USA). The crystallographic structures of CSNP and formulated gCSNP were acquired on a Rigaku Ultima MiniFlex 600 X-ray diffractometer (Rigaku, Germany) using 119 Cu $K\alpha$ radiation operating at 40 kV and 15 mA.

In vitro studies to evaluate the effect of engineered nanoparticles on NLRP3 inflammasome-activated cervical adenocarcinoma cell line (HeLa 229) model

HeLa 229 cell line was procured from the National Centre for Cell Science, Pune and the passage No. 102 was used in the present study. Cells were maintained in DMEM (Gibco, India) supplemented with 10% fetal bovine serum (Gibco, India) and 1% penicillin–streptomycin (Merck, India) at 37 °C in 5% CO_2 humidified incubator (Thermo Fisher Scientific, India).

Cytotoxicity assay

MTT Cell Growth Assay (CT02, Merck, India) was used for assessing the 24-h cytotoxicity of CSNP and gCSNP on HeLa 229 and normal kidney cells (HEK293) cell lines. The cytotoxicity assay was used only as a reference for dose selection of the engineered nanoparticles since the selected doses were used for a time duration limited to 5 h as per the present study design.

Drug treatment

HeLa 229 cells were stimulated with lipopolysaccharide (LPS) obtained from *Escherichia coli* 0111: B44 (Merck, India) at the start of experiment and ATP (Merck, India) was added after 3.5 h of incubation at 37 °C in 5% CO_2 humidified incubator. The test nanoparticles were administered in three doses (0.6 $\mu\text{g}/\text{ml}$ (CSNP1/gCSNP1), 6 $\mu\text{g}/\text{ml}$ (CSNP2/gCSNP2) and 12 $\mu\text{g}/\text{ml}$ (CSNP3/gCSNP3)) along with LPS and harvested after 4.5 h from the start of the experiment.

Relative mRNA expression of genes coding for activated NLRP3 inflammasome complex in cervical cancer cell line

The total RNA was extracted from HeLa 229 cells homogenized in TRI-Reagent (T9424, Merck, India) following the manufacturer's protocol. The extracted RNA was carefully assessed for its quality, purity and integrity using the 260/280 ratio, 260/230 ratio obtained from BioSpectrometer basic, (613500009, Eppendorf, India)

and agarose gel electrophoresis (intact gel bands corresponding to 28S and 18S RNA), respectively. The extracted RNA from each group was diluted to 180 ng/ μ l using nuclease-free water to ensure a known amount of starting mRNA concentration from every group for cDNA synthesis. High-capacity reverse transcriptase cDNA synthesis kit (ThermoFisher Scientific India Pvt. Ltd., India) was used to prepare cDNA (final volume of 20 μ l) from the extracted total RNA using thermocycler (Mastercycler X50, Eppendorf, India). Synthesis of cDNA involved the use of random primers from the cDNA synthesis kit with internal controls as + RT/-RT (with or without reverse transcriptase) to reduce experimental errors. TaqMan™ 20X Assay probes (Table 1; ThermoFisher Scientific, India) were mixed with Universal PCR Master Mix (4304437, Applied Biosystems™, ThermoFisher Scientific, India) for the qPCR experiments. Quantitative polymerase chain reaction (qPCR) was performed in CFX96 (BioRad, India) to assess the relative change in mRNA expression of genes coding for activated NLRP3 inflammasome complex proteins. The PCR conditions used were as follows: to achieve a maximum of the reaction, conditions used were optimized for 20 μ l of the reaction volume with initial denaturation step (hold at 95 °C for 10 min) followed by 40 cycles of 95 °C for 15 s, 60 °C (TaqMan 20X assay specific) for 1 min followed by a final hold at 4 °C.

On completion, the plates were stored at – 20 °C and the mean cycle quantification (Cq) values were recorded (Bustin et al. 2009). Fluorescence signals were detected in the channel 1: Fam (CFX96, Bio-Rad, India). The efficiency of the gene assay mixes was determined using standard dilution method following MIQE guidelines (Bustin et al. 2009). The recorded Cq values from the test group was normalized against efficiency of assay 20X for each gene, sample mRNA amount, number of experimental repeats, number of qPCR repeats and with Cq values of three selected reference genes that were most stably expressed across all experiments. Relative expression of genes for the test groups was compared with that of control and represented by converting to their \log_2 Cq value.

Estimation of secreted IL-1 β

Quantitative ELISA was performed with the Human IL-1 β ELISA Kit (BMS224-2, Invitrogen, India) following manufacturer's instructions using ELISA reader (iMark microplate reader, BioRad, India). This method was used to estimate the secreted IL-1 β present

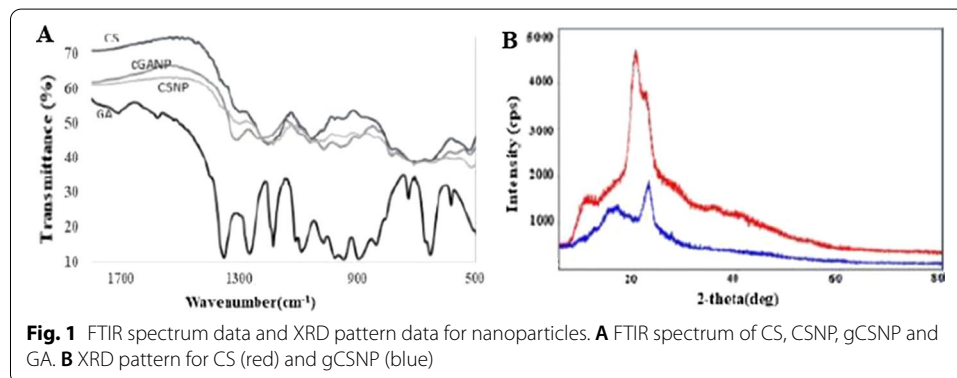
Table 1 TaqMan catalogue number for genes used in the qPCR experiments

Gene name	Catalogue number (TaqMan code)
Hypoxanthine phosphoribosyltransferase 1 (HPRT1)	Hs02800695_m1
Actin beta (ACTB)	Hs01060665_g1
Glyceraldehyde-3-phosphate dehydrogenase (GAPDH)	Hs02786624_g1
NLR family pyrin domain containing 3 (NLRP3)	Hs00918082_m1
PYD and CARD domain containing (PYCARD)	Hs01547324_gH
Caspase 1 (CASP1)	Hs00354836_m1
Purinergic receptor P2X 7 (P2RX7)	Hs00175721_m1
Interleukin 1 beta (IL-1 β)	Hs01555410_m1

Table 2 Size distribution of the NPs as determined by the zeta sizer

CH%	Ch:TPP	GA (mg/gCH)	ZP (mV)	Diameter	PDI	PEE
0.25	1:5	–	58.1	155.1	0.4	
0.25	1:5	50	78.1	181.1	0.35	90.2

The percentage encapsulation off gCSNP has also been computed



in the supernatants of NLRP3 inflammasome-stimulated HeLa 229 cells for every test groups and control.

Statistical analysis

All experiments were performed in triplicates and statistical significance of variation was determined using One-way ANOVA with appropriate post hoc test using GraphPad Prism software version 8.04 for Windows (GraphPad Software, San Diego, California USA) and GeneX 7.0 (GeneX™, Sweden). A value of $p < 0.05$ was considered significant.

Results

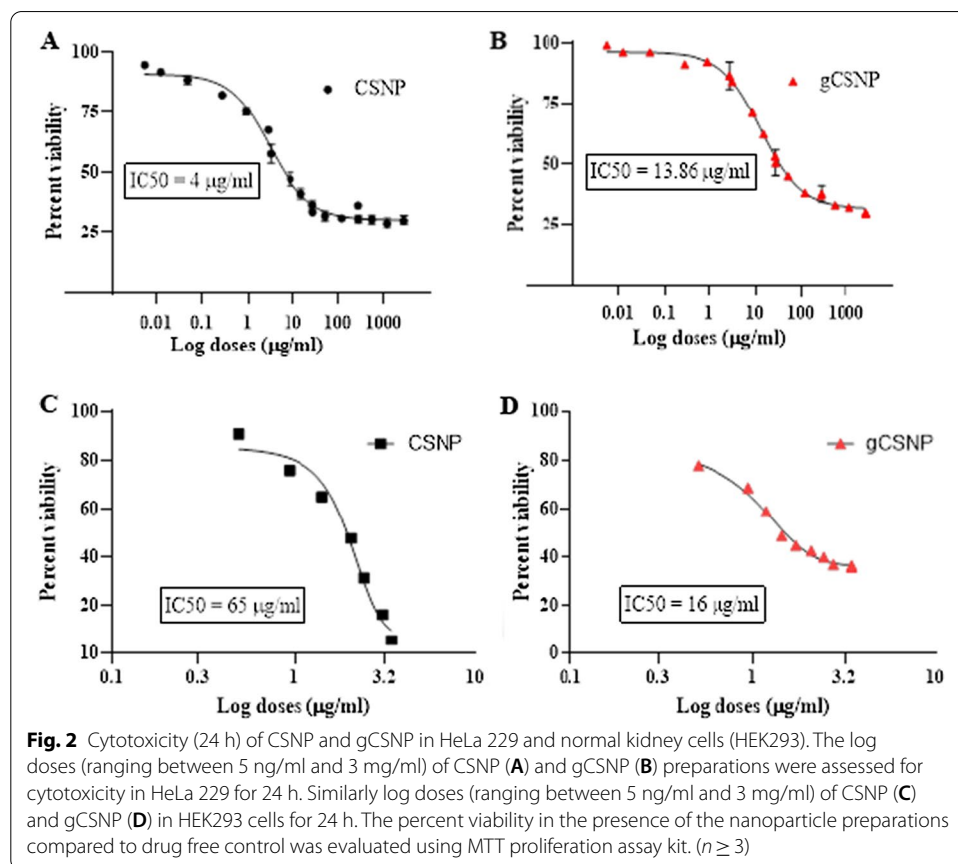
Preparation and characterization of nanoparticles

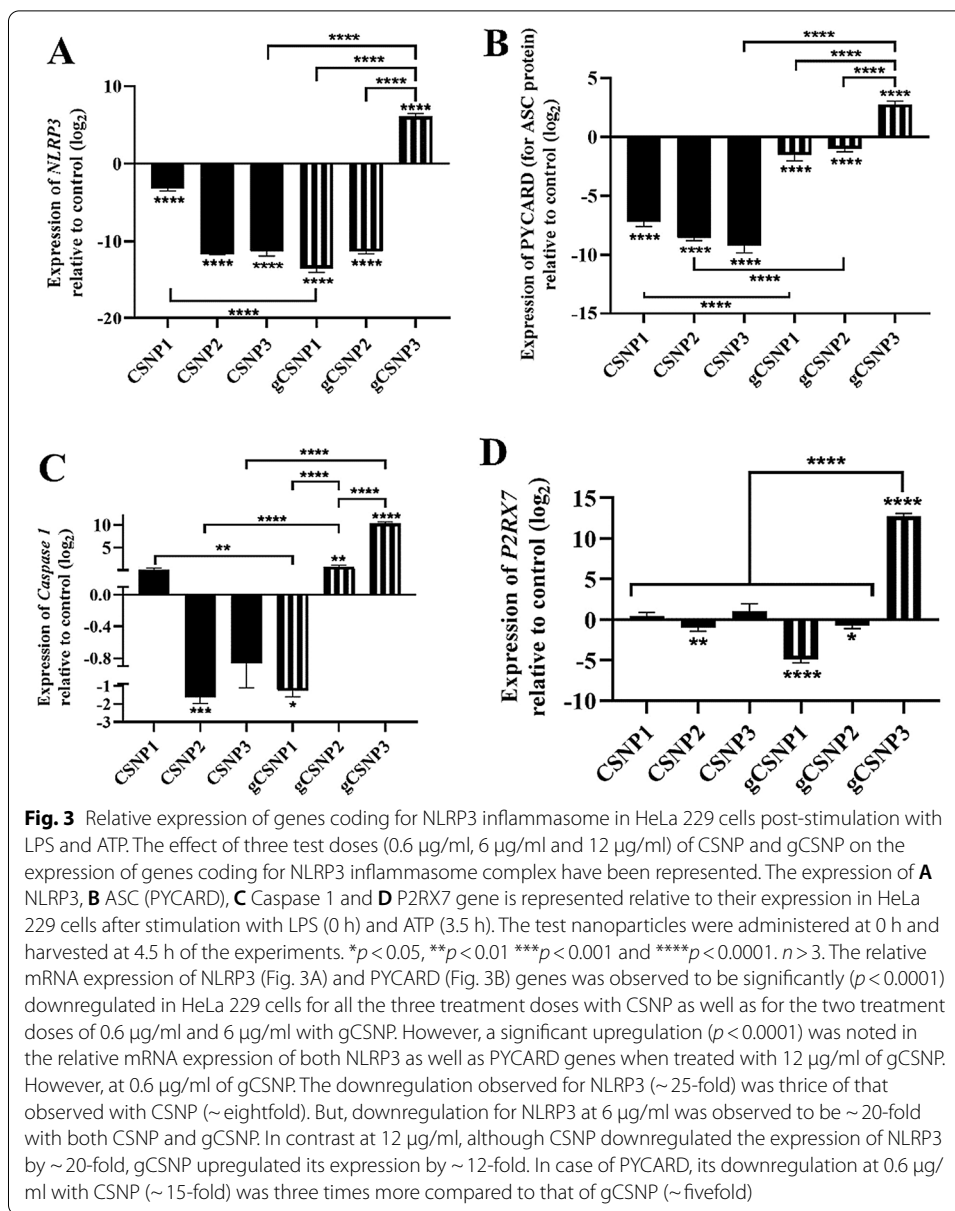
The CSNP and gCSNP were fabricated by ion gelation method using TPP as the cross-linker. The physicochemical characteristics were estimated initially with the zeta sizer to establish the protocol for the size distribution of the nanoparticles. Table 2 summarizes the zeta sizer profile of the nanoparticles prepared by the ion gelation protocol. The size of CSNP was 155.1 ± 5.7 nm in diameter while the size of gCSNP was 181.1 ± 6.9 nm in diameter. The polydispersity index of both the NPs was between 0.35 and 0.4 ± 0.03 . The NPs were later subjected to FTIR and XRD detection protocols to ascertain the conjugation and the structure of the NP (Fig. 1). Since the FTIR spectra between $4000\text{--}2500\text{ cm}^{-1}$ and $1000\text{--}400\text{ cm}^{-1}$ for all the samples were identical, these regions were not plotted. In the FTIR, the spectra of gCSNP were compared with those of CSNP, chitosan (CS) and GA. The FTIR spectra of the CS and its CSNPs revealed a new trough peak indicating the appearance of PO stretching at 1256 cm^{-1} . The FTIR of CS was also compared with gCSNP. The characteristic transmittance trough of CS appeared at 1640, 1585, 1374 and $1150\text{--}1040\text{ cm}^{-1}$. In addition, significant changes in the troughs of amide III group around 1374 cm^{-1} could

be observed. The gCSNPs displayed a decrease in the peak at 1320 and 1380 cm^{-1} . Moreover, the intensity of (NH_2) trough band at 1628 cm^{-1} found in CS decreased dramatically and a new band at 1550 cm^{-1} appeared denoting the cross-linking with TPP during the nanoparticle formation. The FTIR of CS was also compared with gCSNP. The characteristic transmittance trough of CS appeared at 1640, 1585, 1374 and 1150–1040 cm^{-1} . In addition, significant changes in the troughs of amide III group around 1374 cm^{-1} could be observed. The gCSNP displayed a decrease in the peak at 1320 and 1380 cm^{-1} attributed to the NH bending observed in the glucosamine units and at 1420 cm^{-1} (the symmetric NH_3^+ bending region) when compared with CSNPs. In addition, in gCSNP as compared to the CSNP, some changes in the spectra were observed at 1730 and 1640 cm^{-1} representing C=O stretching in esters and C=O stretch of chitosan amide. The XRD spectrum of CS was compared with gCSNP (Fig. 1B). We observed a shift towards the right side in the case of gCSNP signifying an increase in the amorphous nature of the nanoparticle as compared to the CS.

In vitro cytotoxicity assay of NP in HeLa 229 cells

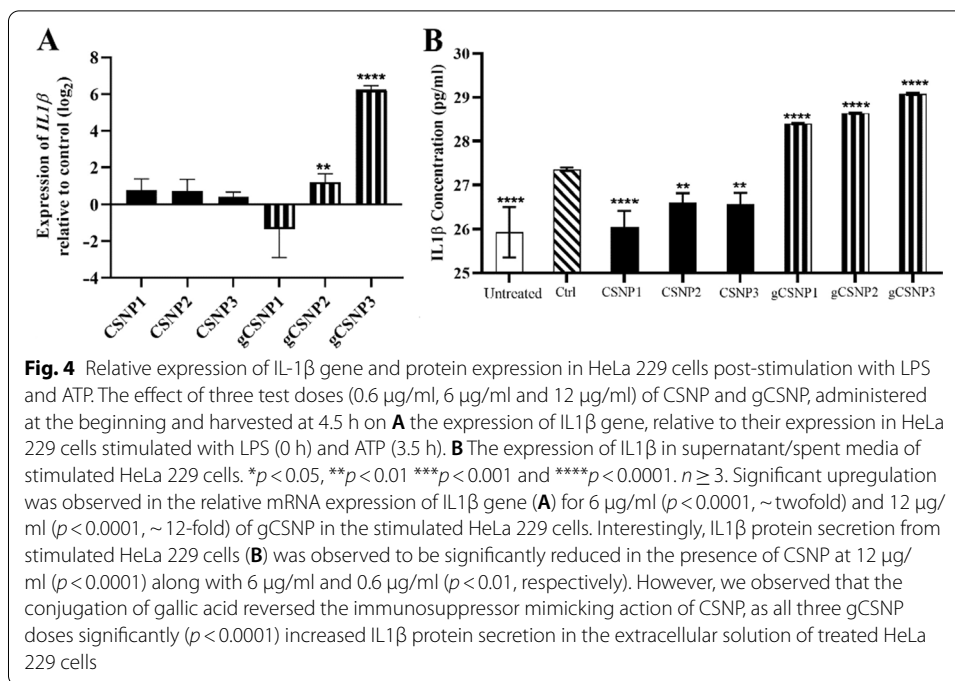
The doses for CSNP and gCSNP were chosen from the linear part of the cytotoxicity dose response curve (Fig. 2) accommodating the 50% viability (IC_{50}) of the HeLa 229





cells after a 24 h incubation. The IC₅₀ of CSNP and gCSNP was recorded to be 4 µg/ml (Fig. 2A) and 13.16 µg/ml (Fig. 2B) and in normal cells (HEK293 cells; IC₅₀ for CSNP 65 µg/ml (Fig. 2C); gCSNP 16 µg/ml (Fig. 2D), respectively, from the non-linear regression of the cytotoxicity curve.

Hence, the effect of three test doses of CSNP and gCSNP on NLRP3 inflammasome-stimulated HeLa 229 cells was assessed (Figs. 3, 4). Figure 3 represents the expression of: (A) NLRP3, (B) PYCARD (for ASC protein), (C) Caspase 1 and (D) P2RX7 genes in the presence of CSNP/gCSNP, relative to control. LPS and ATP was taken as control since significant ($p < 0.001$) increase in ASC gene expression was observed in the presence of both, however neither LPS nor ATP alone produced any additional stimulation of NLRP3 and Caspase1 gene expression (Additional file 1: Figure S1).



The relative mRNA expression of NLRP3 (Fig. 3A) and PYCARD (Fig. 3B) genes was observed to be significantly (*p* < 0.0001) downregulated in HeLa 229 cells for all the three treatment doses (0.6 μg/ml, 6 μg/ml and 12 μg/ml) with CSNP as well as for the two treatment doses of 0.6 μg/ml and 6 μg/ml with gCSNP. However, a significant upregulation (*p* < 0.0001) was noted in the relative mRNA expression of both NLRP3 as well as PYCARD genes when treated with 12 μg/ml of gCSNP. We observed that downregulation for NLRP3 at 0.6 μg/ml of gCSNP (~25-fold) was thrice of that observed with CSNP (~eightfold). However, downregulation for NLRP3 at 6 μg/ml was observed to be ~20-fold with both CSNP and gCSNP. In contrast at 12 μg/ml, although CSNP downregulated the expression of NLRP3 by ~20-fold, gCSNP upregulated its expression by ~12-fold. In case of PYCARD, its downregulation at 0.6 μg/ml with CSNP (~15-fold) was three times more compared to that of gCSNP (~fivefold). Similarly, downregulation for PYCARD at 6 μg/ml was observed to be 4 times more with CSNP (~17-fold) when compared to gCSNP (~fourfold). In contrast at 12 μg/ml, although CSNP further downregulated the expression of PYCARD by ~20-fold, gCSNP upregulated its expression by ~fivefold. The Caspase 1 gene (Fig. 3C) showed nominal variation in its relative mRNA expression. At a dose of 0.6 μg/ml, significant downregulation was observed only with gCSNP (*p* < 0.05, ~2.6-fold). Significant downregulation was observed with CSNP at 6 μg/ml (*p* < 0.001, ~2.6-fold) and 12 μg/ml (*p* < 0.05, ~2.5-fold), although a significant upregulation was noted when treated with gCSNP for the two doses of 6 μg/ml (*p* < 0.001, ~1.6-fold) and 12 μg/ml (*p* < 0.0001, ~20-fold). Similar results were noted in case of the relative mRNA expression of P2RX7 gene (Fig. 3D) in the stimulated HeLa 229 cells with significant downregulation observed when treated with 6 μg/ml of CSNP (*p* < 0.01, ~twofold) and only 0.6 μg/ml of gCSNP (*p* < 0.001, ~tenfold). However, for the highest concentration (12 μg/ml) of gCSNP, there was significant (*p* < 0.001, ~25-fold) upregulation observed in the relative mRNA expression of P2RX7 gene.

Significant upregulation was observed in the relative mRNA expression of IL1 β gene (Fig. 4A) for 6 $\mu\text{g/ml}$ ($p < 0.0001$, ~twofold) and 12 $\mu\text{g/ml}$ ($p < 0.0001$, ~12-fold) of gCSNP in the stimulated HeLa 229 cells. Interestingly, IL1 β protein secretion from stimulated HeLa 229 cells (Fig. 4B) was observed to be significantly reduced in the presence of CSNP at 12 $\mu\text{g/ml}$ ($p < 0.0001$) along with 6 $\mu\text{g/ml}$ and 0.6 $\mu\text{g/ml}$ ($p < 0.01$, respectively).

However, we observed that the conjugation of gallic acid reversed the immunosuppressor mimicking action of CSNP, as all three gCSNP doses significantly ($p < 0.0001$) increased IL1 β protein secretion in the extracellular solution of treated HeLa 229 cells.

Discussion

Inflammasomes are the multi-protein platform in the innate immune system that induce procaspase-1 activation and inflammatory cytokines maturation such as IL1 β . Chitosan-based nanoparticles are good immune enhancers by dint of being able to reverse cytokine changes in immunosuppression preclinical models (Mudgal et al. 2019). To explore the efficacy of the nanoparticles as immunomodulators in the HeLa 229 cell line, we fabricated CSNP and gCSNP. The fabrication of the chitosan nanoparticles and the conjugation of gallic were analyzed with the FTIR. The FTIR spectra of the CS and its CSNPs revealed a new trough peak indicating the appearance of PO stretching at 1256/cm. The characteristic transmittance trough of CS appeared at 1640, 1585, 1374 and 1150–1040 cm^{-1} . This corresponds to amide I, amide II, amide III groups, and glycosidic linkage (C–O–C), respectively (Pawlak and Mucha 2003). Moreover, the intensity of (NH₂) trough band at 1628/cm found in CS decreased dramatically and a new band at 1550/cm appeared. This confirmed the cross-linking of the TPP with chitosan to form the nanoparticles. The FTIR of CS was also compared with gCSNP. The characteristic transmittance trough of CS appeared at 1640, 1585, 1374 and 1150–1040 cm^{-1} . In addition, significant changes in the troughs of amide III group around 1374 cm^{-1} could be observed (Wei and Gao 2016). Amide III bands arose from the C–N stretching vibration. This might be due to the conjugation of GA to the amino group in CS in gCSNP (Wei and Gao 2016). The gCSNP displayed a decrease in the peak at 1320 and 1380/cm attributed to the NH bending observed in the glucosamine units and at 1420/cm (the symmetric NH₃⁺ bending region) when compared with CSNPs. The conjugation of GA with CS was also confirmed by XRD which revealed an increase of amorphous characteristic due to a reduction of the inter- and intra-hydrogen bonds. This is in agreement with the results by other groups (Pasanphan et al. 2008; Pasanphan and Chirachanchai 2008). The size of the engineered nanoparticles is another factor which determines the bio–nano interaction (Nel et al. 2006). The size effect of ENMs on NLRP3 inflammasome activation has been examined with the nanoparticles in the lower range showing pronounced effects on IL-1 β production by several studies, though contradictory results were obtained (Sun et al. 2013). The effect of the size on the NLRP3 inflammasome regulation was studied with CSNP and gCSNP. The size of CSNP was found to be 155 nm while the encapsulation of GA increased the size by 26 nm to 181.1 nm. The encapsulation efficiency of GA was found to be 90.2% based on the already reported earlier (Lamarra et al. 2016).

Activation of NLRP3 inflammasome involves coordinated processes between stimuli and cells. The nanoparticles were fabricated based on the hypothesis that CSNP due

to improved surface area would act as antioxidant curbing the NLRP3 inflammasome and its activity would be further augmented by gallic acid conjugation. Three different models have been proposed for the NLRP3 inflammasome activation. In the present paper, we have tried to explore the K^+ efflux model (Tschopp and Schroder 2010). In the context of the present study, the CSNP induced downregulation of NLRP3 inflammasome complex genes in cervical cancer cells, might prove beneficial in ameliorating the adverse effects of inflammasome gene expression thus avoiding the ensuing adjacent normal tissue damage. Thus, this immunosuppressor mimicking activity of CSNP can potentially inhibit the infiltration of myeloid and myeloid derived cells, thereby preventing the development of inflammatory microenvironment around cancer cells to attenuate tumor progression (Mudgal et al. 2019).

Through our study, we infer that the conjugation of gallic acid reversed the immunosuppressor mimicking action of CSNP, indicated by the release of pro-inflammatory cytokine $IL1\beta$ from HeLa 229 cells. It is known that gallic acid and CSNP work synergistically as is observed in our study where in contrast to CSNP alone, gCSNP upregulated the expression of genes coding for NLRP3 inflammasome pathway as part of the priming signal (Hamarsheh and Zeiser 2020; Mudgal et al. 2019; Zheng et al. 2018). Hence, we infer that CSNP alone at 155 nm size, downregulated the expression of genes coding for NLRP3 inflammasome complex even at higher doses. The present study demonstrated how a bifunctional role of CSNP can be elicited with the mere conjugation of gallic acid, by reversing its role in HeLa 229 cells. This allowed an unopposed priming signal for the inflammasome complex proteins. This effect on the priming signal by gCSNP could be due to the physicochemical property of the nanoparticle and its interaction with the biological system that is occurring at the nano-bio interface.

Furthermore, with respect of the activation signal, our study helps to infer that unlike gCSNP, CSNP was also effective in controlling the formation of NLRP3 inflammasome complex probably by inhibiting the P2RX7 gene even in the presence of external ATP as per the K^+ efflux model (Hamarsheh and Zeiser 2020; Kantono and Guo 2017; Karki and Kanneganti 2019). The significant increase in the $IL1\beta$ secretion from HeLa 229 cells when treated with gCSNP indicate that conjugating gallic acid led to the reversal of drug action. To the best of our knowledge, we demonstrated for the first time that conjugation of gallic acid reverses the immunosuppressor mimicking property of CSNP in NLRP3 inflammasome-stimulated HeLa 229 cell line model. We can speculate within reason that the conjugation of gallic acid with CSNP could potentially activate the NLRP3 inflammasome as previously observed with other NPs by Jo et al. 2016. In the presence of higher doses of gCSNP, the increased $IL1\beta$ release from cervical cancer cells accompanied with the upregulation of P2RX7 gene implicated the unopposed activation of NLRP3 inflammasome complex.

Conclusions

The present study demonstrated that the role reversal of CSNP can be achieved when conjugated with gallic acid at higher doses. Interestingly, given its wide range of safe limits of cytotoxicity, as observed in our study, alternative administration time can be tested to come to a conclusion in case of HeLa 229 cells. Additionally, on a larger perspective, it is an interesting finding to note that gallic acid conjugated nanoparticles

have the potential to act as an immunomodulator as is indicated by the upregulation of IL1 β . However, the limitation of this study involves the lack of experimental data demonstrating the interaction of NLRP3, ASC, Caspase 1 and P2RX7 proteins subsequent to the effect of the NPs on HeLa 229 cell line model. Furthermore, the metabolic consequences of tumor microenvironment influencing the cancer hallmark of immune evasion in the context of the present study, would unravel important information regarding the role of the NPs.

Hence, future research coupling the protein expression along with the gene expression of the genes coding for the NLRP3 inflammasome complex in treated HeLa 229 cell line model can reveal the immunomodulatory mechanism of CSNP which may have its translational significance as potential treatment strategies for cancer.

Abbreviations

CSNP: Chitosan nanoparticle; gCSNP: Gallic acid conjugated chitosan nanoparticle; GA: Gallic acid; LPS: Lipopolysaccharide; ATP: Adenosine triphosphate; ENM: Engineered nano-materials.

Supplementary Information

The online version contains supplementary material available at <https://doi.org/10.1186/s12645-021-00090-y>.

Additional file 1: Figure S1. Relative expression of genes coding for NLRP3 inflammasome complex proteins in the presence of LPS &/or ATP. The relative expression of ASC coding gene was significantly higher in the presence of LPS in combination with ATP. *** $p < 0.001$. $n > 3$.

Acknowledgements

We thank Linda Bobby Tholath and Jesna Suresh (MIT, MAHE) for their assistance with the cytotoxicity assays. The authors would also like to thank MIT, MAHE for the infrastructure help and MAHE for funding the research work.

Authors' contributions

RR designed the experimental protocols, performed synthesis and characterization of the nanoparticles and performed cell culture analytical experiments and the results analysis of the samples. RC and UB designed the experimental protocols, performed the experiments and did the results analysis of the cell culture experiments. GP performed the experiments of the cell culture. SRBS contributed in maintaining the cell culture. RR, RC, UB and BSSR contributed to writing the manuscript. All authors reviewed the final draft of the manuscript. All authors read and approved the final manuscript.

Funding

The work was carried out under the Seed Grant Scheme (Grant No. 00000387) awarded by MAHE, Manipal, to conduct the experiments.

Availability of data and materials

The data will be available if needed.

Declarations

Ethics approval and consent to participate

Not applicable.

Consent for publication

All authors agree with the publication of this manuscript in this journal.

Competing interests

The authors declare that there is no conflict of interest.

Author details

¹Department of Microbiology, Melaka Manipal Medical College, Manipal Academy of Higher Education, Manipal 576104, Karnataka, India. ²Department of Biotechnology, Manipal Institute of Technology, Manipal Academy of Higher Education, Manipal 576104, Karnataka, India. ³Directorate of Research, Manipal Academy of Higher Education, Manipal 576104, Karnataka, India. ⁴Department of Pharmacology, Melaka Manipal Medical College, Manipal Academy of Higher Education, Manipal 576104, Karnataka, India. ⁵Manipal Center for Infectious Diseases, Prasanna School of Public Health, Manipal Academy of Higher Education, Manipal 576104, Karnataka, India.

Received: 2 April 2021 Accepted: 2 July 2021

Published online: 11 August 2021

References

- Ainsworth EA, Gillespie KM. Estimation of total phenolic content and other oxidation substrates in plant tissues using Folin-Ciocalteu reagent. *Nat Protoc.* 2007;2(4):875–7.
- Arbyn M, Weiderpass E, Bruni L, de Sanjosé S, Saraiya M, Ferlay J, et al. Estimates of incidence and mortality of cervical cancer in 2018: a worldwide analysis. *Lancet Glob Heal.* 2020;8(2):e191–203. [https://doi.org/10.1016/S2214-109X\(19\)30482-6](https://doi.org/10.1016/S2214-109X(19)30482-6).
- Bryant C, Fitzgerald KA. Molecular mechanisms involved in inflammasome activation. *Trends Cell Biol.* 2009;19(9):455–64.
- Bustin SA, Benes V, Garson JA, Hellemans J, Huggett J, Kubista M, et al. The MIQE guidelines: minimum information for publication of quantitative real-time PCR experiments. *Clin Chem.* 2009;55(4):611–22.
- Calvo P, Remuñan-López C, Vila-Jato JL, Alonso MJ. Chitosan and chitosan/ethylene oxide-propylene oxide block copolymer nanoparticles as novel carriers for proteins and vaccines. *Pharm Res.* 1997;14(10):1431–6.
- Hamarshah S, Zeiser R. NLRP3 inflammasome activation in cancer: a double-edged sword. *Front Immunol.* 2020;11:1444.
- Jo E-K, Kim JK, Shin D-M, Sasakawa C. Molecular mechanisms regulating NLRP3 inflammasome activation. *Cell Mol Immunol.* 2016;13(2):148–59.
- Kantono M, Guo B. Inflammasomes and cancer: the dynamic role of the inflammasome in tumor development. *Front Immunol.* 2017;8:1132.
- Karki R, Kanneganti T-D. Diverging inflammasome signals in tumorigenesis and potential targeting. *Nat Rev Cancer.* 2019;19(4):197–214.
- Kruger S, Ilmer M, Kobold S, Cadilha BL, Endres S, Ormanns S, et al. Advances in cancer immunotherapy 2019—latest trends. *J Exp Clin Cancer Res.* 2019;38(1):268. <https://doi.org/10.1186/s13046-019-1266-0>.
- Lamarra J, Rivero S, Pinotti A. Design of chitosan-based nanoparticles functionalized with gallic acid. *Mater Sci Eng C.* 2016;67:717–26.
- Lamarra J, Giannuzzi L, Rivero S, Pinotti A. Assembly of chitosan support matrix with gallic acid-functionalized nanoparticles. *Mater Sci Eng C.* 2017;79:848–59.
- Mishra GA, Pimple SA, Shastri SS. Prevention of cervix cancer in India. *Oncology.* 2016;91(Suppl 1):1–7.
- Moossavi M, Parsamanesh N, Bahrami A, Atkin SL, Sahebkar A. Role of the NLRP3 inflammasome in cancer. *Mol Cancer.* 2018;17(1):158. <https://doi.org/10.1186/s12943-018-0900-3>.
- Mudgal J, Mudgal PP, Kinra M, Raval R. Immunomodulatory role of chitosan-based nanoparticles and oligosaccharides in cyclophosphamide-treated mice. *Scand J Immunol.* 2019;89(4): e12749. <https://doi.org/10.1111/sji.12749>.
- Nel A, Xia T, Mädler L, Li N. Toxic potential of materials at the nanolevel. *Science.* 2006;311(5761):622–7.
- Park W, Heo YJ, Han DK. New opportunities for nanoparticles in cancer immunotherapy. *Biomater Res.* 2018. <https://doi.org/10.1186/s40824-018-0133-y>.
- Pasanphan W, Chirachanchai S. Conjugation of gallic acid onto chitosan: an approach for green and water-based antioxidant. *Carbohydr Polym.* 2008;72(1):169–77.
- Pasanphan W, Buettner GR, Chirachanchai S. Chitosan conjugated with deoxycholic acid and gallic acid: a novel biopolymer-based additive antioxidant for polyethylene. *J Appl Polym Sci.* 2008;109(1):38–46.
- Pawlak A, Mucha M. Thermogravimetric and FTIR studies of chitosan blends. *Thermochim Acta.* 2003;396(1):153–66.
- Pontillo A, Bricher P, Leal VNC, Lima S, Souza PRE, Crovella S. Role of inflammasome genetics in susceptibility to HPV infection and cervical cancer development. *J Med Virol.* 2016;88(9):1646–51. <https://doi.org/10.1002/jmv.24514>.
- Sun W. Recent advances in cancer immunotherapy. *J Hematol Oncol.* 2017;10(1):96. <https://doi.org/10.1186/s13045-017-0460-9>.
- Sun B, Wang X, Ji Z, Li R, Xia T. NLRP3 inflammasome activation induced by engineered nanomaterials. *Small.* 2013;9(9–10):1595–607.
- Tschopp J, Schroder K. NLRP3 inflammasome activation: the convergence of multiple signalling pathways on ROS production? *Nat Rev Immunol.* 2010. <https://doi.org/10.1038/nri2725>.
- Wei Z, Gao Y. Evaluation of structural and functional properties of chitosan-chlorogenic acid complexes. *Int J Biol Macromol.* 2016;86:376–82.
- Zheng M, Zhang C, Zhou Y, Lu Z, Zhao H, Bie X, et al. Preparation of gallic acid-grafted chitosan using recombinant bacterial laccase and its application in chilled meat preservation. *Front Microbiol.* 2018;9:1729.

Publisher's Note

Springer Nature remains neutral with regard to jurisdictional claims in published maps and institutional affiliations.

Ready to submit your research? Choose BMC and benefit from:

- fast, convenient online submission
- thorough peer review by experienced researchers in your field
- rapid publication on acceptance
- support for research data, including large and complex data types
- gold Open Access which fosters wider collaboration and increased citations
- maximum visibility for your research: over 100M website views per year

At BMC, research is always in progress.

Learn more biomedcentral.com/submissions

